genus *Orsodacne* [J. S. Mann and R. A. Crowson, *J. Nat. Hist.* **15**, 727 (1981)]. Although the larval affiliations of *Orsodacne* are still unconfirmed, these are probably in the male strobili of Pinaceae (with which all eight species co-occur), a resource available during the early spring flights of the pollen-feeding adults.
19. The belid subfamily Allocoryninae comprises >20 species in the Neotropical genus *Rhopalotria*, which attack the male strobili of *Zamia* and *Dioon*.
20. The chrysomelid subfamily Aulacoscelidinae comprises 18 species in two Neotropical genera restricted to the Cycadaceae.
21. L. Brundin, *Evolution* **19**, 496 (1965).
22. G. Kuschel, in *Australian Weevils*, E. Zimmerman, Ed. [Commonwealth Scientific and Industrial Research Organization (CSIRO), Melbourne, Australia, 1994], p. 569. Other nemonychids in the Karatau Formation apparently belong to the now-extinct subfamily Brenthorrhininae (*9*). The Nemonychidae are also represented by *Libanorhinus succinus* in Lower Cretaceous amber derived from Araucariaceae resins [G. Kuschel and G. O. Poinar, *Entomol. Scand. (Group 2)* **24**, 143 (1993)] and by the Lower Cretaceous *Slonik* in the central Asian trans-Baikal deposits [G. Kuschel, *GeoJournal* **7**, 499 (1983)].
23. The oxycorynine *Archeorrhynchus paradoxopus* (Belidae) is found in the Karatau Formation [G. Kuschel, in *Australian Weevils*, E. Zimmerman, Ed. (CSIRO, Melbourne, Australia, 1994), p. 244]. Oxycoryninae are also represented in the Lower Cretaceous Santana Formation of Brazil [D. A. Grimaldi, Ed., *Bull. Am. Mus. Nat. Hist.* **195**, 8 (1990)]. Additional Karatau belids include the extinct subfamily Eobelinae [V. V. Zherikhin and V. G. Gratshev, in *Biology and Classification of Coleoptera: Papers Celebrating the 80th Birthday of Roy A. Crowson*, J. Pakaluk and S. A. Slipinski, Eds. (Muzeum I Instytut Zoologi PAN, Warsaw, 1995), p. 646].
24. The belid subfamily Carinae, which attacks strobili of the coniferous Cupressaceae, occurs in the Jurassic Karatau beds, as represented by *Eccoptarthrus* and *Emanrhynchus* [V. V. Zherikhin and V. G. Gratshev, in *Biology and Classification of Coleoptera: Papers Celebrating the 80th Birthday of Roy A. Crowson*, J. Pakaluk and S. A. Slipinski, Eds. (Muzeum I Instytut Zoologi PAN, Warsaw, 1995), pp. 634–777]. The Carinae also appear in the Lower Cretaceous trans-Baikal beds (*Cretonanophyes* and Baissorhynchus); the Carinae presently contains *Car*, which is found in Australia and Tasmania, and *Chilecar* and *Caenominurus*, which are found in Chile and Argentina [E. Zimmerman, Ed., *Australian Weevils* (CSIRO, Melbourne, Australia, 1994), p. 504.
25. The chrysomelid *Cerambyomima longicornis*, attributed to the Aulacoscelinae [G. Kuschel and B. M. May, *Invertebr. Taxon.* **3**, 697 (1993)], resembles the orsodacnine *Cucujopsis* in the grooved frons and may be an intermediate form.
26. Jurassic fossil cones of *Araucaria mirabilis* from Argentina closely resemble *A. bidwellii* and show damage similar to that caused by weevil larvae [see R. A. Stockey, *Paleontographica* **166**, 1 (1978)]. *A. bidwellii* is host to extant species in both the Nemonychidae and Palophaginae.
27. R. A. Stockey, *J. Plant Res.* **107**, 493 (1994).
28. B. D. Farrell, D. Dussourd, C. Mitter, *Am. Nat.* **138**, 881 (1991).
29. The allocorynine *Scelocamptus curvipes* is found in the Karatau beds (*10*).
30. The aulacosceline genera *Protoscelis*, *Protosceloides*, and *Pseudomegamerus* are found in the Karatau beds (*5*).
31. T. N. Taylor and E. L. Taylor, *The Biology and Evolution of Fossil Plants* (Prentice-Hall, Englewood Cliffs, NJ, 1993).
32. P. R. Ehrlich and P. H. Raven, *Evolution* **18**, 586 (1964); B. D. Farrell and C. Mitter, *Biol. J. Linn. Soc.* **68**, 533 (1998).
33. J. Jernvall, J. P. Hunter, M. Fortelius, *Science* **274**, 1489 (1996).
34. Assignments of feeding habits and numbers of recent genera are from Lawrence (*6*).
35. The number of genera was extracted from the totals per beetle family in Lawrence (*6*).
36. Estimates of diversity are from the following sources: Curculionoidea (*7*); Chrysomelidae [P. Jolivet, E. Petitpierre, T. H. Hsiao, Eds., *Biology of Chrysomelidae* (Kluwer Academic, Dordrecht, Netherlands, 1988)]; Cerambycidae [S. Bily and O. Mehl, *Longhorn Beetles (Coleoptera, Cerambycidae) of Fennoscandia and Denmark*, vol. 22 of *Fauna Entomologica of Scandinavica* (Brill, Leiden, Netherlands, 1989)].
37. For a discussion of the use of fossils to assign character optimizations, see J. M. Doyle and M. J. Donoghue, *Rev. Palaeobot. Palynol.* **50**, 63 (1987).
38. For supplying specimens or identifications of key or austral taxa, I especially thank F. Andrews, J. Chemsak, L. Diego-Gomez, J. Donaldson, C. Duckett, T. Erwin, W. Flowers, D. Furth, C. D. Johnson, J. Kingsolver, G. Kuschel, J. Lawrence, A. Newton, K. Norstog, R. Oberprieler, C. O'Brien, and E. G. Riley, among many others. I also thank A. Salmore, M. Blair, and L. Morrissey for technical lab support; A. Berry, M. Donoghue, D. Futuyma, A. Knoll, D. Lewontin, E. Mayr, C. Mitter, N. Moran, B. Normark, S. Palumbi, N. Pierce, and E. O. Wilson for helpful discussions; and A. Knoll, C. Labandeira, and D. Maddison for detailed comments on a late draft. This research was supported by NSF, USDA, and the Putnam Expedition Fund of the Museum of Comparative Zoology.

19 January 1998; accepted 8 June 1998

Activity-Dependent Cortical Target Selection by Thalamic Axons

Susan M. Catalano* and Carla J. Shatz†

Connections in the developing nervous system are thought to be formed initially by an activity-independent process of axon pathfinding and target selection and subsequently refined by neural activity. Blockade of sodium action potentials by intracranial infusion of tetrodotoxin in cats during the early period when axons from the lateral geniculate nucleus (LGN) were in the process of selecting visual cortex as their target altered the pattern and precision of this thalamocortical projection. The majority of LGN neurons, rather than projecting to visual cortex, elaborated a significant projection within the subplate of cortical areas normally bypassed. Those axons that did project to their correct target were topographically disorganized. Thus, neural activity is required for initial targeting decisions made by thalamic axons as they traverse the subplate.

During the wiring of connections between the thalamus and cortex in mammals, there is an intermediate step in which thalamic axons grow and interact with a special population of neurons—subplate neurons—before they contact their ultimate target neurons within the cortical plate (*1*, *2*). For example, LGN axons en route to visual cortex emit transient side branches that extend into the subplate under both target and nontarget cortical areas (*3*) and form functional synaptic contacts with subplate neurons (*4*). During this period of development, spontaneous action potential activity generated in the retina and relayed through the LGN likely drives these subplate synapses in vivo (*5*). Thus, synaptic relations within the subplate could support activity-dependent interactions during the process of thalamocortical axon target selection.

To examine if activity is needed for thalamic axons to form connections with their appropriate cortical target area, we infused tetrodotoxin (TTX, a sodium channel antagonist that blocks action potentials) or vehicle through osmotic minipumps (*6*) into the brain of cat fetuses between E42 (E42 = 42 days of gestation) and E56. At E42, the first LGN axons have just reached the subplate underneath visual cortex but still have side branches along their trajectory. Between E42 and E50, the majority of LGN axons have arrived in the visual subplate; by E56, many have departed the subplate and reached their ultimate target, layer 4 of the cortical plate (*3*). To assess the consequences of the treatments on the thalamocortical projection, we injected carbocyanine dyes at E56 to label retrogradely LGN neurons (*7*) and subsequently counted the numbers of neurons sending axons to the subplate or cortical plate of either visual (the correct target) or auditory (an incorrect target) cortex.

The number of LGN neurons projecting to visual cortex was decreased in TTX-infused animals (Fig. 1), both within the subplate [Fig. 1C; an average of 69 ± 5% SEM fewer neurons than vehicle controls, $n = 8$ animals; 4 littermate pairs treated with TTX or vehicle and matched for similar 1,1′-dioctadecyl-3,3,3′,3′-tetramethylindocarbocyanine perchlorate (DiI) injection sizes] and within the cortical plate (Fig. 1C; 94 ± 0.5% SEM, $n = 8$ animals; 4

Howard Hughes Medical Institute and Department of Molecular and Cell Biology, University of California, Berkeley, CA 94720–3200, USA.

*Present address: Division of Biology, 216-76, California Institute of Technology, Pasadena, CA 91125, USA. E-mail: scatalan@cco.caltech.edu

†To whom correspondence should be addressed. E-mail: cshatz@socrates.berkeley.edu

littermate pairs treated with TTX or vehicle and matched for similar DiI injection sizes) (*8*). However, the overall development of the LGN itself was relatively unaffected (compare Fig. 1, A and B). Previous studies have shown that the dendritic and somatic development of LGN neurons also proceeds essentially normally during the entire treatment period (*9*), although we noted a modest decrease in the size of the LGN [size of TTX-treated LGN is 76 ± 5% of that of vehicle-treated LGN, n = 3 littermate pairs (6 animals)].

The intracortical pathway normally taken by LGN axons en route to visual cortex bypasses many cortical areas, including auditory cortex. Thus, we examined whether, after TTX treatment, LGN neurons send axons to the subplate or cortical plate of auditory cortex rather than to visual cortex (Fig. 1D). In vehicle-treated cases at E56, relatively few LGN neurons could be retrogradely labeled after 1,1′-dioctadecyl-3,3,3′,3′-tetramethylindodicarbocyanine perchlorate (DiD) injections into the subplate or cortical plate of auditory cortex. The largest dye injection (covering 9.6 mm^3 of the cortical plate and subplate of A1) labeled only 354 LGN neurons; a similarly sized dye placement in V1 labeled 4345 LGN neurons. After TTX treatment, fewer LGN axons could be retrogradely labeled by an injection of DiD into auditory cortex proper (Fig. 1D; 75 ± 6% SEM, n = 4 animals; 2 littermate pairs treated with TTX or vehicle and matched for similar DiD injection sizes). However, in TTX-treated animals, there was a substantial increase in the number of LGN neurons retrogradely labeled after tracer injections into the subplate underlying auditory cortex (Fig. 1D; 437 ± 189% SEM; n = 4 animals; 2 littermate pairs treated with TTX or vehicle and matched for similar DiD injection sizes) (*10*). Thus, blockade of action potential activity apparently alters the spatial patterning of the geniculocortical projection by derailing many LGN axons into the subplate underlying auditory cortex.

To visualize directly the aberrant routing of LGN axons within the subplate, we injected DiI into the LGN to label the axons anterogradely. In vehicle-treated animals (Fig. 2A; n = 2 animals), as in unmanipulated littermates at E56 (n = 2) (*3*, *11*), LGN axons were tightly fasciculated in the optic radiations but branched extensively within visual subplate and visual cortex; few, if any, side branches were given off as LGN axons passed by other cortical areas. In contrast, axons in TTX-treated littermates (n = 2) extended many branches in the subplate of nonvisual areas along their entire route to visual cortex (Fig. 2B, arrowheads), and few axons actually made it as far as V1. This experiment confirms the conclusion inferred from the retrograde labeling experiments that TTX treatment alters the spatial patterning of the projection from the LGN to cortex.

Two additional aspects of the geniculocortical projection were also perturbed after TTX treatment. Many LGN axons within the cortical plate of V1 fail to arborize within cortical layer 4 and instead send unbranched projections up into the pial surface (*12*). Here we report that the topography of the projection to visual cortex was also degraded after TTX treatment (Fig. 3). This degraded topography is evident when comparing the spatial distribution of retrogradely labeled neurons after similarly located and sized DiI injections into visual cortex (Fig. 3A; n = 8 TTX-vehicle littermate pairs): Neurons were more dispersed across the LGN in the TTX-treated cases than in the vehicle-treated cases (*13*). The portion of total LGN covered by labeled neurons was consistently larger in the TTX-infused brains than in those of vehicle-treated controls (Fig. 3B) (average 52 ± 8% SEM in TTX brains versus 28 ± 2% in control brains; n = 4 TTX-vehicle littermate pairs; $P < 0.01$, Student's t test). There was also more variability in the location of the peak number of retrogradely labeled neurons within the LGN in TTX-treated animals (*14*). These results suggest that the topographic map of those LGN neurons that did manage to project to visual cortex is significantly degraded; regions of the LGN that would normally not project to a given cortical location at E56 did so in TTX-treated animals. Thus, thalamocorti-

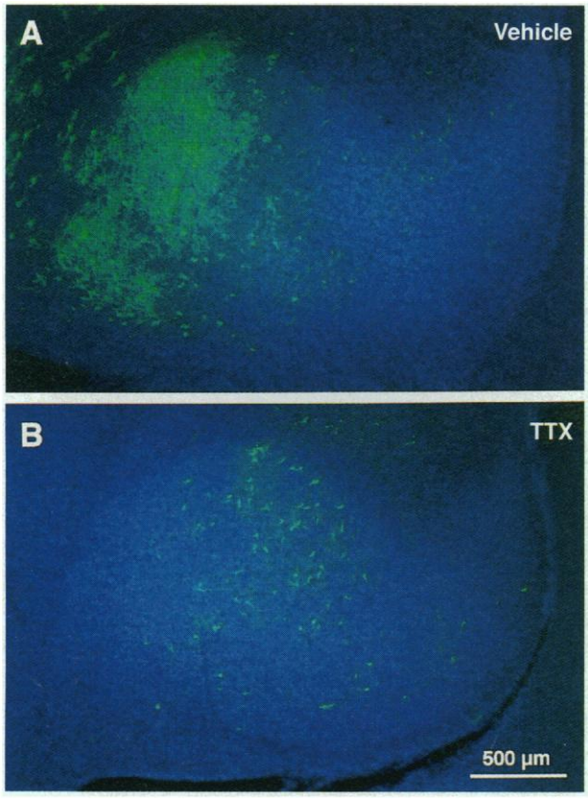

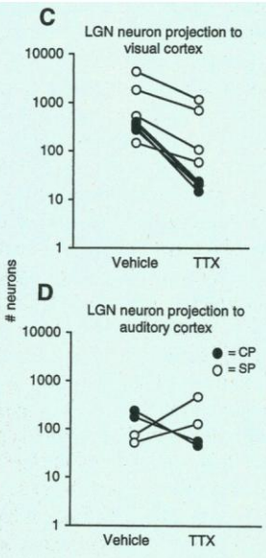

Fig. 1. The number of LGN neurons projecting to visual cortex is markedly decreased after intraventricular infusion of TTX between E42 and E56 (*6*). For assessment of the consequences of the treatment, DiI was placed into the cortical plate or subplate of visual or auditory areas at E56 to label neurons retrogradely within the LGN, and the number of labeled LGN neurons was counted (*7*). All data are from littermate pairs treated with either TTX or vehicle and also matched for similarly sized dye injections in cortex or subplate. LGN neurons from a vehicle-treated (**A**) or TTX-treated (**B**) littermate pair were retrogradely labeled after injection of DiI in the visual cortex (green cells in these fluorescence photomicrographs). Despite similarly sized and located DiI injections, the TTX-treated animal has far fewer LGN neurons projecting to the visual cortex than the vehicle-infused littermate. Scale bar (A and B), 500 μm. The number of LGN neurons labeled after dye placements in either the cortical plate (CP, filled dots) or subplate (SP, open dots) of visual cortex (**C**) or auditory cortex (**D**) is plotted on a logarithmic scale. Individual littermate pairs treated with either TTX or vehicle and matched for dye injection size are pictured as pairs of connected dots. The range of counts reflects the sizes of the dye injections [for example, in (C), the largest matched injections labeled 4345 LGN neurons in a vehicle-treated fetus but only 1153 in a TTX-treated littermate]; comparisons should be made between littermate pairs [n = 8 littermate pairs for (C) and 4 littermate pairs for (D)]. Note the decrease in numbers of LGN neurons projecting to visual cortex and visual subplate (C) and the increase in numbers projecting to auditory subplate (D).

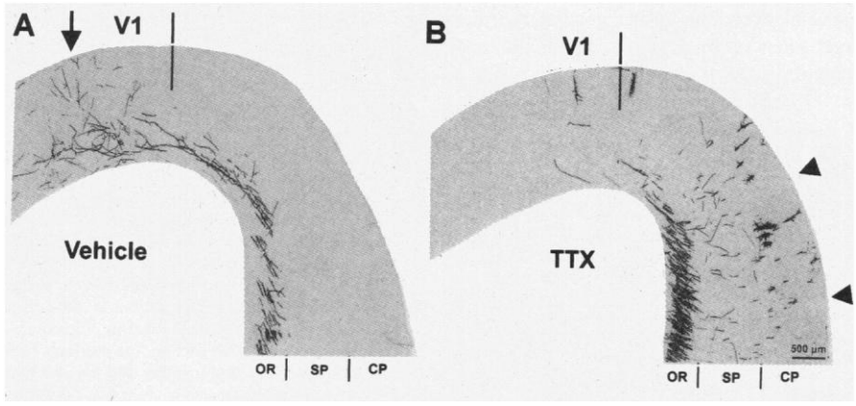

Fig. 2. After activity blockade, LGN axon growth and arborization in the visual cortex are reduced, and branching en route within the subplate is increased. (**A**) Anterograde labeling of axons from injection of DiI in LGN reveals that, in vehicle-treated animals, axons navigate normally to primary visual cortex (V1) and selectively branch within visual subplate and cortical plate (arrow). As LGN axons traverse nonvisual areas, they remain fasciculated in the optic radiations. (**B**) In TTX-treated littermates, LGN axons growing within the optic radiations extend many branches into the subplate of nonvisual areas (arrowheads). Their growth into visual cortex is diminished relative to vehicle-treated controls. Visual cortex (V1) is located left of the vertical bars at the top of each panel. Laminar divisions of neocortex are indicated at the bottom of each panel (OR, optic radiations; SP, subplate; CP, cortical plate).

cal connections, like retinotectal connections (*15*), must use both activity-independent and activity-dependent mechanisms in the refinement of topographic projections within their target area.

The results of this study argue for a requirement for action potential activity in the decision-making that occurs as growing thalamic axons traverse the subplate en route to their appropriate cortical target areas. How might activity operate in the targeting of LGN axons? We think it unlikely that TTX acts simply to "freeze" LGN axons into the projection pattern present at the time of onset of the TTX infusion. At E56, even after TTX treatments, the number of LGN neurons projecting to visual cortex increased threefold over the projection at E42 (n =3 untreated animals at E42 compared with n = 3 TTX-treated animals at E56) (*16*). In addition, at E42 the side branches present along the route of LGN axons were few and short (*3*), whereas in the TTX-treated cases at E56 branching was extensive. There was also extensive growth of the dendrites and somata of LGN neurons after similar TTX treatment (*9*). These considerations indicate that LGN axons are not "frozen" in the immature state present at E42.

The results of our experiments, on the contrary, argue that activity blockade alters the pattern of axonal branching, and therefore the targeting decisions, of LGN axons rather than growth per se. The decrease in the number of LGN neurons projecting to visual cortex and subplate and the accompanying increase in the number projecting to nonvisual subplate, including that of auditory cortex, can be explained if side branches that would normally be eliminated between E42 and E56 instead grow when action potentials are blocked. This suggestion is consistent with the known effects of similar treatments on the growth and branching of axons in many other developing systems, including the mammalian retinogeniculate and retinocollicular pathways and the retinotectal system of fish and frogs (*17*, *18*).

Few LGN axons managed to grow all the way back to the visual cortex when activity was blocked between E42 and E56. Indeed, the subplate along the entire intracortical trajectory of LGN axons may be available as a valid intermediate target for LGN axons in the absence of action potential activity. It may be that once LGN axons arborize within the subplate underlying inappropriate cortical regions, they are no longer able to respond to cues along the pathway that would promote continued growth toward visual cortex (*19*). Despite the targeting errors, the directionality of LGN axon growth—toward the posterior pole of the cortex—is not perturbed by TTX treatment, consistent with the hypothesis that positional information guiding axon pathfinding can be read by thalamocortical axons in an activity-independent manner. Cues may include the Eph family of receptors and ligands, which are known to subserve such functions in the developing retinotectal system of vertebrates (*20*).

The subplate appears to be a crucial decision-making compartment in which dynamic interactions between growing thalamic axons and subplate cells ultimately result in the selection of the correct cortical target area (*21*). Our results argue for a requirement for activity-dependent interactions in the initial steps of cortical target selection by thalamic axons. It is unclear at present whether these interactions enable growing axons to select directly the appropriate target (instructive) or simply to read specific target-derived molecular cues (permissive). Whatever the mechanism, the formation of connections between thalamus and neocortex in mammals may be

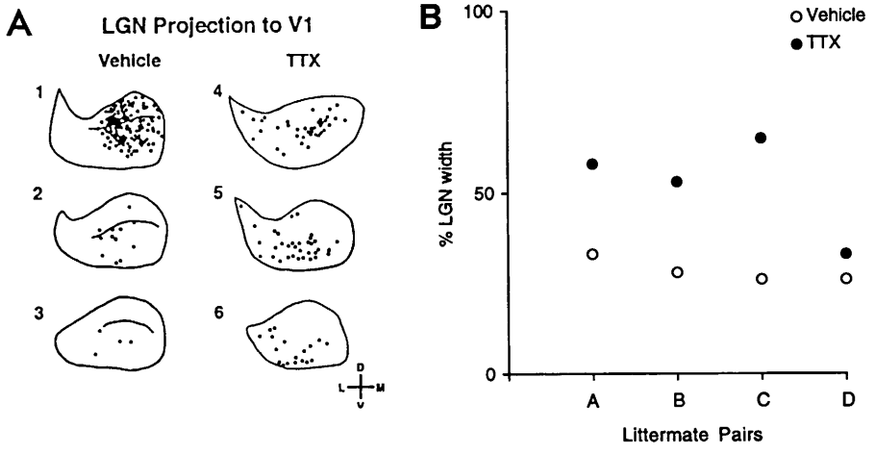

Fig. 3. Precision of topography in the LGN projection to visual cortex is degraded after activity blockade. (**A**) The location of LGN neurons retrogradely labeled from comparably sized and located DiI injections into visual cortex is plotted within an outline of the LGN of vehicle-treated (1 to 3) or TTX-treated (4 to 6) animals in comparable sections. The altered distribution of labeled neurons within the LGN of TTX-treated animals is apparent (see also Fig. 1, A and B). Orientation of sections marked by arrows; M, medial; L, lateral; D, dorsal; V, ventral. (**B**) Neurons projecting to a given location in V1 are distributed over a small percentage of the total width of LGN in vehicle-treated animals (28 ± 2% SEM; open circles); however, in TTX-treated animals (closed circles), neurons covering a much larger percentage of the total LGN width (52 ± 8% SEM; $P < 0.01$) project to a comparable location in V1. Sections shown in (A) were some of those used to calculate values for the littermate pairs "A" of Fig. 3B. See (*13*).

a special exception to the general rule that target selection by developing axons is independent of neural activity.

References and Notes

1. C. S. Goodman and C. J. Shatz, *Neuron* **10**, 77 (1993); C. J. Shatz and D. D. M. O'Leary, *Arch. Ophthalmol.* **111**, 472 (1993); L. C. Katz and C. J. Shatz, *Science* **274**, 1133 (1996).
2. K. L. Allendoerfer and C. J. Shatz, *Annu. Rev. Neurosci.* **17**, 185 (1994); N. Konig, G. Roch, R. Marty, *Anat. Embryol.* **148**, 73 (1975); D. Kristt, *ibid.* **157**, 217 (1979); I. Kostovic and P. Rakic, *J. Neurocytol.* **9**, 219 (1980); F. Valverde, M. Facal-Valverde, M. Santacana, M. Heredia, *J. Comp. Neurol.* **290**, 118 (1989).
3. A. Ghosh and C. J. Shatz, *J. Neurosci.* **12**, 39 (1992).
4. E. Friauf, S. K. McConnell, C. J. Shatz, *ibid.* **10**, 2601 (1990); K. Herrmann, A. Antonini, C. J. Shatz, *Eur. J. Neurosci.* **6**, 1729 (1994).
5. E. Friauf and C. J. Shatz, *J. Neurophysiol.* **66**, 2059 (1991); R. Wong, M. Meister, C. J. Shatz, *Neuron* **11**, 923 (1993); R. Mooney, A. Penn, R. Gallego, C. J. Shatz, *ibid.* **17**, 863 (1996).
6. All animal care was in accordance with institutional guidelines. A total of 25 fetuses (E56, $n = 22$; E42, $n = 3$) were studied from pregnant cats in our breeding colony of known gestational age. Anesthesia, sterile surgical techniques, and minipump implantations were according to (*22*). After infusion of either 300 μM TTX or vehicle (300 μM sodium citrate buffer) between E42 and E56, the fetuses were delivered by cesarean section and were transcardially perfused (*3*). Fetuses are always studied as littermate pairs (TTX-treated compared with vehicle-treated) because TTX diffuses throughout the entire forebrain and midbrain bilaterally (*9*), and therefore it is not possible to compare hemispheres in the same animal.
7. Crystals of DiI (D-282, Molecular Probes, Eugene, OR) were placed into either the subplate or cortical plate of visual cortex to label LGN neurons that project there or into the LGN itself to visualize the axonal projection from LGN to cortex. In the same animals, crystals of DiD (D-7757, Molecular Probes) were also placed into the region of auditory cortex to label LGN axons that might extend collaterals into this region on their way back to visual cortex. After 3 months for dye diffusion, brains were sectioned horizontally on a vibratome at 100 μm, and retrogradely labeled LGN neurons were counted. Because the number of retrogradely labeled neurons is directly proportional to the size of the dye injection site, great care was taken to make similar dye injection sizes for each TTX- and vehicle-treated littermate pair ($n = 11$ matched littermate pairs studied). The variations in total neuron number seen in Fig. 1, C and D, reflect differing size injections, and therefore comparisons can only made between matched littermate pairs.
8. Infusion of vehicle did not have an apparent effect on the magnitude of the LGN projection to visual cortex; the number of retrogradely labeled LGN neurons was within 10% (± 2% SEM, $n = 3$ unmanipulated and 3 vehicle-treated; $P < 0.005$) of untreated littermate controls matched for similar injection sizes.
9. Previous studies have demonstrated that intracranial minipump infusions of TTX produce concentrations that are sufficient to block sodium-dependent action potentials bilaterally throughout the entire forebrain and midbrain at E42 to E56 (*22*) and result in the failure of retinal ganglion axons to segregate into eye-specific layers in the LGN (*17, 23*). However, many other aspects of development proceed normally: Cell migration and cell division within the cortex are unimpaired, the brain grows to normal size during the treatment period and its gross histological organization is indistinguishable from normal (*23*), and the somatic and dendritic development of retinal ganglion cells and LGN neurons is normal [(*22*); M. Dalva, A. Ghosh, C. J. Shatz, *J. Neurosci.* **14**, 3588 (1994)]. Moreover, the development of cortical pyramidal cell dendrites, radial glial cells, and the overall appearance and thickness of the cortical plate is indistinguishable from normal (*12*).
10. TTX infusions were begun at E42, after large numbers of MGN axons had already invaded the auditory cortical plate [A. Ghosh and C. J. Shatz, *Development* **117**, 1031 (1993)].
11. S. M. Catalano and C. J. Shatz, data not shown.
12. K. Herrmann and C. J. Shatz, *Proc. Natl. Acad. Sci. U.S.A.* **92**, 11244 (1995).
13. TTX- or vehicle-treated littermate pairs with small dye placements (2 to 3 mm^3) in identical cortical locations were analyzed for topographic precision ($n = 4$ pairs) (Fig. 3). The location of individual labeled LGN neurons with respect to the borders of the LGN was marked on digitized images of sections. The mediolateral distribution of marked neurons within a single section was plotted in 100-μm bin widths (NIH Image version 1.61). This procedure was repeated for every LGN section. The distributions for all sections were added together, and the peak number of retrogradely labeled neurons was determined. Finally, the percentage of total mediolateral width of LGN covered by labeled neurons at half-peak was derived and plotted in Fig. 3B.
14. The peak in the number of retrogradely labeled neurons was located near the center of LGN in vehicle-treated animals (within 250 to 300 μm of the center of LGN), consistent with dye placements within the corresponding locations in visual cortex. However, in TTX-treated animals, the peak was located further medially in two cases and further laterally in one case (550 to 350 μm away from the center) than in vehicle-treated control littermates, even though the DiI injections were similarly placed in cortex, suggesting that there is more variability in the overall topography of the geniculocortical projection after TTX treatment.
15. J. T. Schmidt and M. Buzzard, *J. Neurobiol.* **21**, 900 (1990); U. Drescher *et al.*, *Cell* **82**, 359 (1995); M. Nakamoto *et al.*, *ibid.* **86**, 755 (1996).
16. The normal increase between E42 and E56 in the number of LGN neurons projecting to visual cortex, as determined by retrograde labeling with DiI injections, is about 30-fold ($n = 3$ untreated animals at E42 and 3 vehicle-treated animals at E56).
17. D. W. Sretavan, C. J. Shatz, M. P. Stryker, *Nature* **336**, 468 (1988).
18. D. K. Simon, G. T. Prusky, D. D. M. O'Leary, M. Constantine-Paton, *Proc. Natl. Acad. Sci. U.S.A.* **89**, 10593 (1992); H. Cline, *Trends Neurosci.* **14**, 104 (1991); M. D. Olson and R. L. Meyer, *J. Neurosci.* **14**, 208 (1994).
19. It is conceivable that TTX somehow disrupts cortical differentiation, which in turn affects LGN axon targeting and ingrowth. Although this disruption is possible, we note that many aspects of cortical development can proceed normally after similar TTX treatments; see (*9*).
20. M. Tessier-Lavigne, *Cell* **82**, 345 (1995).
21. A. Ghosh, A. Antonini, S. K. McConnell, C. J. Shatz, *Nature* **347**, 179 (1990); Z. Molnar and C. Blakemore, *ibid.* **351**, 475 (1991); J. A. De Carlos and D. D. M. O'Leary, *J. Neurosci.* **12**, 1194 (1992); J. Bolz, N. Novak, V. Staiger, *ibid.*, p. 3054.
22. G. Campbell, A. S. Ramoa, M. P. Stryker, C. J. Shatz, *Visual Neurosci.* **14**, 779 (1997).
23. C. J. Shatz and M. P. Stryker, *Science* **242**, 87 (1988).

24. We thank A. Raymond and D. Escontrias for help with the fetal surgeries. Supported by NIH grant EY02838 (C.J.S.) and National Research Service Award EY06491 (S.M.C.). S.M.C. is an Associate and C.J.S. is an Investigator of the Howard Hughes Medical Institute.

12 March 1998; accepted 10 June 1998

A Viral Mechanism for Inhibition of the Cellular Phosphatase Calcineurin

James E. Miskin, Charles C. Abrams, Lynnette C. Goatley, Linda K. Dixon*

The transcription factor NFAT (nuclear factor of activated T cells) controls the expression of many immunomodulatory proteins. African swine fever virus inhibits proinflammatory cytokine expression in infected macrophages, and a viral protein A238L was found to display the activity of the immunosuppressive drug cyclosporin A by inhibiting NFAT-regulated gene transcription in vivo. This it does by binding the catalytic subunit of calcineurin and inhibiting calcineurin phosphatase activity.

Viruses encode many proteins that interfere with host defense systems (*1*). Nucleotide sequence analysis of the African swine fever virus (ASFV) genome (*2*) identified genes encoding proteins that are potentially able to interfere with the host response to viral infection. These include A238L, which has sequence similarity with IκB, and prevents activation of nuclear factor kappa B (NF-κB)–dependent gene transcription (*3*). The similarity between A238L and IκB is limited to the central region of the protein, which contains three ankyrin-like repeats. The NH_2- and COOH-terminal regions of A238L are unlike those of the cellular IκB proteins (*4*), indicating that A238L may function by means of a mechanism different from that of IκB.

To identify host proteins with which A238L interacts, we used the yeast two-hybrid system (*5, 6*) to screen a cDNA library from pig alveolar macrophages. Nine clones specifically interacted with A238L, including four containing cDNA encoding the entire porcine cyclophilin A (*CypA*) gene. Another four clones contained cDNAs encoding all but the first 30 to 40 NH_2-terminal amino acid residues of the catalytic (A) subunit of the Ca^{2+}-calmodulin–regulated cellular phospha-

Institute for Animal Health, Pirbright Laboratory, Pirbright, Surrey, GU24 0NF, UK. E-mail: linda.dixon@bbsrc.ac.uk

*To whom correspondence should be addressed.